

## The Teleconnection between the Western Indian and the Western Pacific Oceans

VASUBANDHU MISRA

*Center for Ocean–Land–Atmosphere Studies, Institute of Global Environment and Society, Inc., Calverton, Maryland*

(Manuscript received 3 December 2002, in final form 3 July 2003)

### ABSTRACT

Shown in this study are a teleconnection pattern relating outgoing longwave radiation (OLR) anomalies over the western Pacific Ocean and sea surface temperature anomalies (SSTAs) over the western Indian Ocean over two seasons [September–October–November (SON) and December–January–February (DJF)] at zero lag from observations and atmospheric general circulation model (AGCM) integrations. This teleconnection pattern suggests that a positive SSTA in the SON and DJF seasons over the western Indian Ocean increases the contemporaneous positive OLR anomalies over the western Pacific Ocean. This teleconnection pattern is also simulated by the Center for Ocean–Land–Atmosphere studies (COLA) AGCM forced with observed SST. From the experimental COLA AGCM runs (wherein the Pacific Ocean SST variability is suppressed except for the climatological annual cycle), it is diagnosed that the interannual variability of OLR over the western Pacific Ocean persists because of this teleconnection. This teleconnection pattern is found to be associated with the modulation of the equatorial zonal wind circulation by the western Indian Ocean SSTAs.

### 1. Introduction

In this study we explore the relationship between the western Indian Ocean (WIO) sea surface temperature (SST) variability and outgoing longwave radiation (OLR) variability on interannual time scales over the western Pacific Ocean (WPO) from both atmospheric general circulation model (AGCM) integrations and observations. In the recent past, the relation between the variability of the SST over the Indian Ocean and climate variation elsewhere has been extensively investigated. The influence of the Indian Ocean SST anomalies (SSTAs) on the Indian monsoon has been documented in Shukla (1987), Clark et al. (2000), and Arpe et al. (1998). Meehl (1993, 1987) indicated that both the Indian and Pacific Oceans were actively involved in the evolution of El Niño through the modulation of the tropical biennial oscillation. Similarly, Nicholls (1989), Makarau and Jury (1997), and Latif et al. (1999) have identified the role of Indian Ocean SSTAs on climate variability over Australia, Zimbabwe, and eastern equatorial Africa, respectively.

There are a number of studies that show that Indian Ocean SST is influenced by SSTAs in the eastern Pacific at a lag of a few months (Klein et al. 1999; Venzke et al. 2000; Nicholson 1997). Klein et al. (1999) show that variability in clouds, surface winds, and thereby the

surface fluxes, over the Indian Ocean correspond with SST variability over the Pacific Ocean. Krishnamurthy and Kirtman (2001) indicate that the dipolelike variation in the Indian Ocean SST is largely a manifestation of the El Niño–Southern Oscillation (ENSO) phenomenon, but that it can be excited by processes that are independent of ENSO. Huang and Kinter (2002) show that there is variability in the time period of 2–5 yr in the subsurface tropical Indian Ocean, which is significantly correlated to ENSO variability. Latif and Barnett (1995), using uncoupled atmospheric, oceanic general circulation model experiments, and hybrid coupled model simulations, concluded that ENSO plays a key role in generating interannual variability in all three tropical ocean basins. Furthermore, they found that the local air–sea interactions over the Indian and the Atlantic Oceans amplify the ENSO-induced signals in the ocean and in the atmosphere. They also found that the Indian Ocean has virtually no impact on the evolution of ENSO in the Pacific Ocean.

Some recent studies, however, have also shown that variability of the Indian Ocean may have influence on the variability of the Pacific Ocean. Meehl et al. (1996) show that the subseasonal propagation of convection from the Indian Ocean to the western Pacific ultimately culminates with westerly wind burst events over the western Pacific that serve as a prelude to an evolving ENSO. Curtis et al. (2002), using observations and National Centers for Environmental Prediction (NCEP) reanalysis, identified an eastern equatorial Indian Ocean (EEIO) mode of variability with a periodicity of 2–7 yr. This mode is depicted as a precipitation gradient south

---

*Corresponding author address:* Dr. Vasubandhu Misra, Center for Ocean–Land–Atmosphere Studies, Institute of Global Environment and Society, Inc., 4041 Powder Mill Road, Suite 302, Calverton, MD 20705.

E-mail: misra@cola.iges.org

TABLE 1. The outline of the AGCM used in the study.

Process	Reference
Dynamical core	Kiehl et al. (1998)
Advection	Dependent variables are spectrally treated except for moisture variable, which is advected by semi-Lagrangian scheme.
Time integration	Semi-implicit
Deep convection	Relaxed Arakawa–Schubert scheme; Moorthi and Suarez (1992)
Shallow convection	Tiedke (1984)
Shortwave radiation	Davies (1982); Lacis and Hansen (1974)
Longwave radiation	Harshvardhan et al. (1987)
Boundary layer	Level 2.0 closure; Mellor and Yamada (1982)
Diagnostic cloud fraction and optical properties	Kiehl et al. (1998)
Orography	Smoothed mean (Fennessy et al. 1994)
Land surface process	Xue et al. (1991, 1996)

of Sumatra Island and the central equatorial Indian Ocean. They show that in the 3–4 months following the positive phase of this EEIO mode (with enhanced rainfall over south of Sumatra), there is a surge in the power of 30–60-day oscillation over the region, which has a significant correlation with ENSO events. Kirtman and Shukla (2000), from their coupled ocean–atmosphere modeling study, found that a variable Asian summer monsoon enhances the ENSO variability and can even serve as a trigger mechanism for ENSO. They suggest that in a coupled ocean–atmosphere system, monsoon wind stress anomalies lead to a temporally and spatially remote response of SSTAs over the tropical Pacific via ocean wave dynamics and coupled air–sea interactions.

This study explains the teleconnection pattern between the WIO and the WPO when significant SSTAs establish in the WIO by September–October–November (SON). I ascribe to the idea that there is a synergistic relationship between the Indian and Pacific Oceans, and

the variability in the two ocean basins are equally important to the ultimate evolution of ENSO and ENSO-like variability in the Pacific Ocean.

In the following section the outline of the AGCM used in the study is listed, followed by a description of the design of experiments and datasets used. The interannual variability of the OLR anomaly over the WPO is discussed in section 3a. Subsequently, the teleconnection pattern is described in section 3b, and an explanation for it from the model simulations and observations is provided in section 3c. Finally, conclusions are presented in section 4.

## 2. Design of experiments and datasets

For this study, six ensemble members of the control Center for Ocean–Land–Atmosphere Studies (COLA) AGCM at T42 spectral truncation with 18 levels for 18 yr were run, starting from 0000 UTC 15 December 1978. The details of the model are outlined in Table 1. The atmospheric initial conditions for these ensemble members were generated by initially running the COLA AGCM from NCEP reanalysis for 0000 UTC 15 December 1978 for a week and resetting the date on the restart file to the initial date. This procedure was repeated five more times to obtain synoptically independent atmospheric initial conditions for the other ensemble members. This procedure has been adopted in other past studies (Misra 2003; Kirtman et al. 2001). The surface boundary condition of SST is obtained from the monthly mean of the Hadley Centre Sea Ice and Sea Surface Temperature (HADISST) dataset (Parker et al. 1999). This dataset is available on a  $1^\circ \times 1^\circ$  grid from 1870 to present. The soil moisture fields are obtained from a 2-yr climatology of the Global Soil Wetness Project (Dirmeyer and Zeng 1999).

A set of six additional experimental model runs was conducted using the same initial atmospheric and land

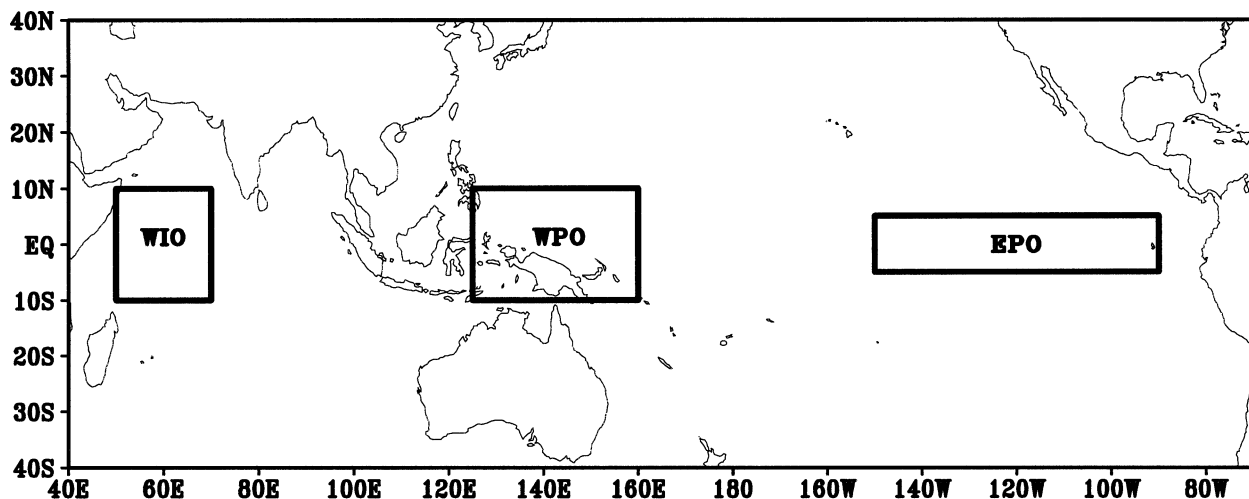


FIG. 1. The domains of the oceanic regions of WIO, WPO, and EPO used in determining the teleconnection patterns.

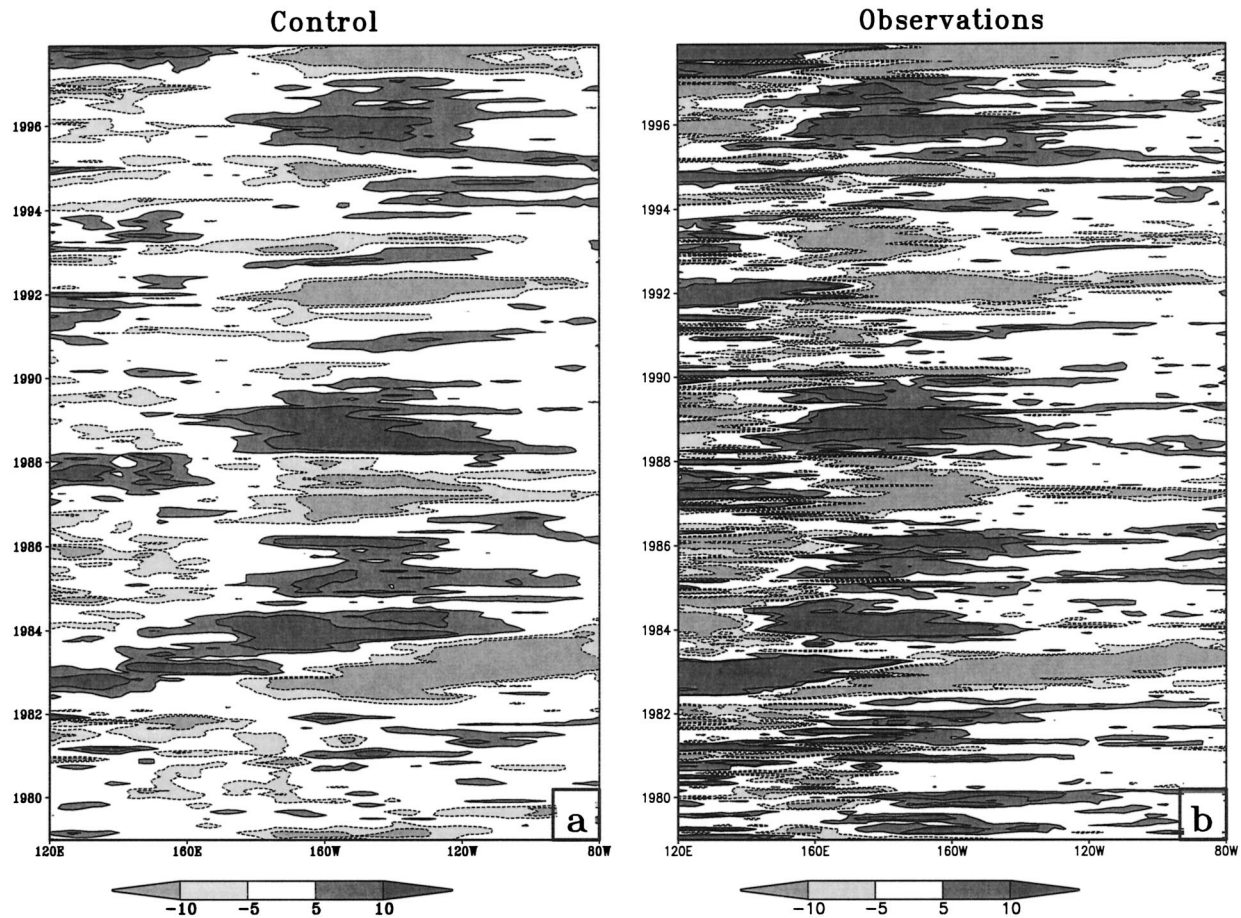


FIG. 2. The OLR anomalies averaged between  $10^{\circ}\text{S}$  and  $10^{\circ}\text{N}$  from (a) the control COLA AGCM and (b) the observations based on Liebmann and Smith (1996). The units are in  $\text{W m}^{-2}$ .

surface conditions as in the control COLA AGCM as above. However, in these experimental runs seasonally varying climatological SST was used over the entire Pacific Ocean, while in the rest of the ocean basins the observed SST was used. The purpose of these experiments is to identify the mechanism of the remote forcing on the WPO rainfall.

To verify some of the results from these model simulations we use the NCEP reanalysis (Kalnay et al. 1996). The model OLR is validated against the observed OLR, which follows Liebmann and Smith (1996) and is obtained as the interpolated OLR dataset from the National Oceanic and Atmospheric Administration–Cooperative Institute for Research in Environmental Sciences (NOAA–CIRES) Climate Diagnostics Center in Boulder, Colorado. This dataset is available on  $2.5^{\circ} \times 2.5^{\circ}$  latitude–longitude grid. It should be mentioned that all results from the model simulation in this study are presented from the ensemble mean.

This study extensively covers the interannual variability during the boreal winter season over the WIO, the WPO, and the eastern Pacific Ocean (EPO). The domains of this region are indicated in Fig. 1. The WIO

domain follows from Krishnamurthy and Kirtman (2001), while that over the EPO is identical to the Niño-3 region ( $5^{\circ}\text{N}$ – $5^{\circ}\text{S}$ ,  $90^{\circ}$ – $150^{\circ}\text{W}$ ) that has the largest variability on ENSO time scales over the tropical Pacific (<http://iri.columbia.edu/climate/ENSO/background/monitoring.html>). The motivation for the domain over the WPO will follow from the discussion in section 3.

### 3. Results

#### a. Interannual variability of western Pacific OLR anomalies

The COLA AGCM has been extensively used for climate simulations (Misra 2003; Straus and Shukla 2002). It has also been successfully coupled to an ocean model that reproduces the present climate reasonably well (Kirtman et al. 2002). In this section the WPO OLR anomalies from the control and experiment AGCM integrations are compared with observations. The intent is to document the reliability of the COLA AGCM in simulating the tropical variability. In Fig. 2a we show the longitude–time cross section of OLR anomalies av-

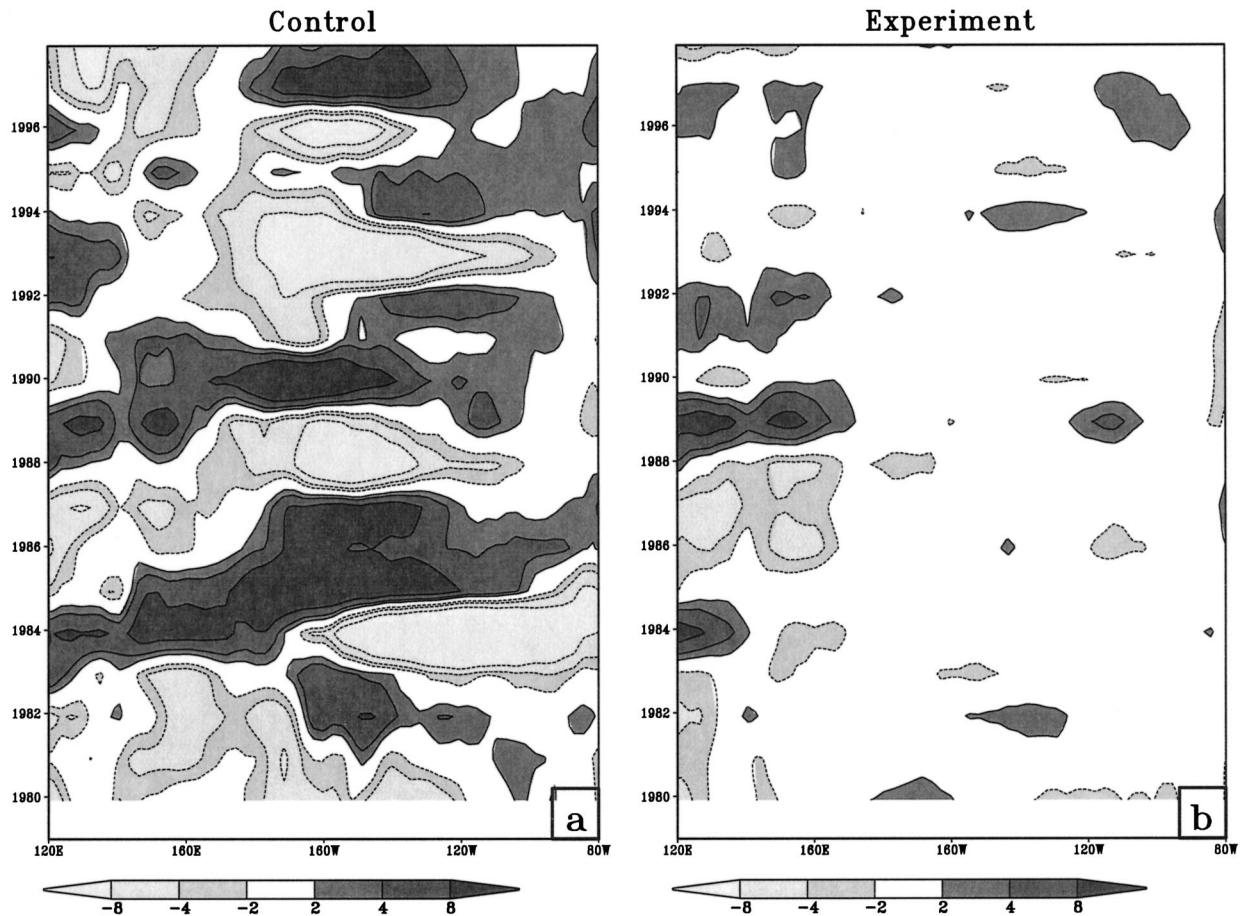


FIG. 3. The DJF OLR anomalies averaged between  $10^{\circ}\text{S}$  and  $10^{\circ}\text{N}$  from the (a) control and (b) experiment COLA AGCM integrations. The units are in  $\text{W m}^{-2}$ .

eraged between  $10^{\circ}\text{S}$  and  $10^{\circ}\text{N}$  and the corresponding observations in Fig. 2b. The interannual variability over the tropical Pacific is reasonably well captured by the model. The warm (cold) ENSO events of 1983/84, 1987/88, 1991/92 (1984/85, 1985/86, 1996/97) with negative (positive) OLR anomalies from Fig. 2a are verifiable in Fig. 2b. However, in the control model integrations, the positive OLR anomalies extend too far to the east. Furthermore, the high-frequency variability is relatively dormant over the WPO, while it is erroneously enhanced over the central and eastern Pacific Ocean.

The motivation for this study came primarily from Figs. 3a and 3b, which show the time-longitude cross section of December–January–February (DJF) OLR anomalies from the control and AGCM experiments averaged between  $10^{\circ}\text{S}$  and  $10^{\circ}\text{N}$ , respectively. It is clearly seen that the experimental run displays an interannual variability west of  $160^{\circ}\text{E}$  that is comparable to that in the control run. Therefore, a domain that best represents this variability over the WPO is indicated in Fig. 1. Furthermore, the time series of the OLR anomalies averaged over this domain from observations and the control in Fig. 4a and from the experimental run in Fig. 4b

are plotted. The control model correlates well with observations, as indicated in Fig. 4a. However, the amplitude of the variability in the control simulation is relatively smaller than in the observations. In Fig. 4b the experimental run also displays an interannual variability that is comparable to the control run, albeit with a smaller amplitude. The goal of this study is to understand the cause of this variability over the WPO in the experimental AGCM run.

#### b. The teleconnection pattern

Krishnamurthy and Kirtman (2001) indicate that there is a lag of about one season in the interannual variability of the monthly mean SSTAs between the WIO and the WPO. Specifically, they indicate that peak variability in SSTAs occurs in SON over the WIO followed by peak variability in DJF over the WPO. Furthermore, we found that the largest interannual anomalies of OLR over the WPO from AGCM control simulations and observations appears in DJF. It is also comparable to SON anomalies in some years (not shown). I was therefore motivated to examine the contemporaneous correlations of rainfall

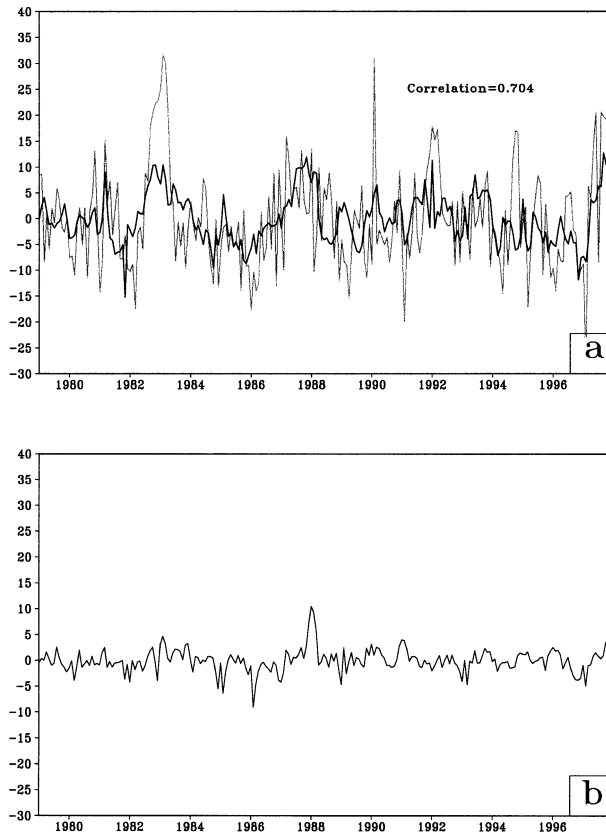


FIG. 4. The time series of OLR anomalies averaged over the western Pacific Ocean (see Fig. 1) from the (a) control (black line) and observations (gray line) and (b) experimental COLA AGCM simulations. The correlation between the two time series in (a) is also shown. The units are in  $W m^{-2}$ .

variability as diagnosed from OLR variations over the WPO with global SSTAs for SON and DJF.

Shown in Figs. 5a and 5b are the contemporaneous correlation significant at a 90% confidence interval according to a two-tailed  $t$  test between the WPO OLR anomalies and global SST for the SON and DJF seasons from the control COLA AGCM simulations, respectively. The teleconnection indicates that an increase (decrease) over the WIO and the EPO (WPO) is accompanied by a simultaneous increase in OLR over the WPO. The teleconnection appears robust in SON over the WIO. In DJF (Fig. 5b) the correlation pattern recedes from the Arabian Sea and appears over the eastern Indian Ocean. These teleconnection patterns were validated from observations in Fig. 6. The observations seem to verify the AGCM simulations, with the teleconnection pattern appearing over the WIO in SON and appearing farther eastward in DJF. However, there are significant differences between the control and observed teleconnection patterns, the foremost being the appearance of relatively much stronger correlations over the WIO in the control in Fig. 5a relative to observations in Fig. 6a. In addition, the absence of the negative cor-

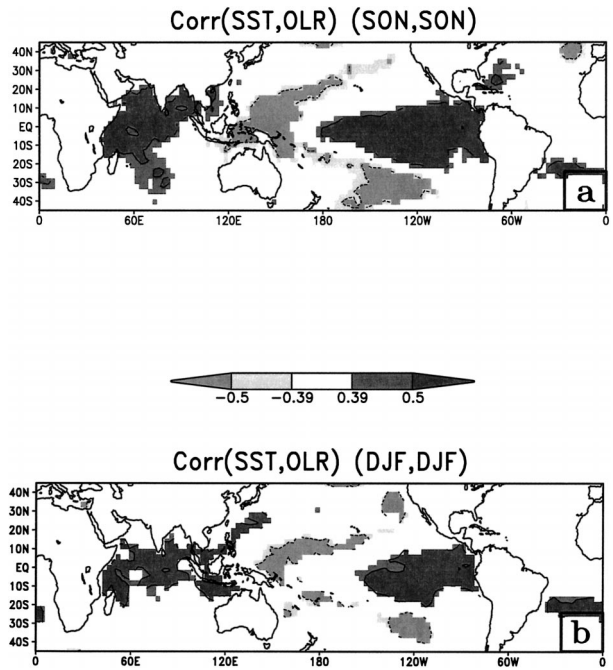


FIG. 5. The contemporaneous correlation of WPO OLR anomalies with global observed SST for (a) SON and (b) DJF from control AGCM simulations. Only significant values at a 90% confidence interval according to a  $t$  test are plotted.

relations over the eastern Indian Ocean in SON and the relative weakening of the teleconnection pattern over the South Pacific convergence zone (SPCZ) region in DJF (Fig. 5b) in the control integrations are not sup-

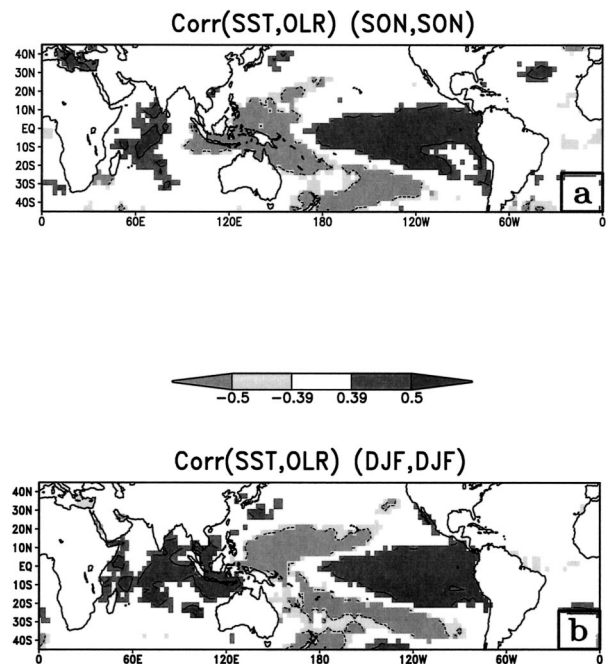


FIG. 6. Same as Fig. 5, but from observations.

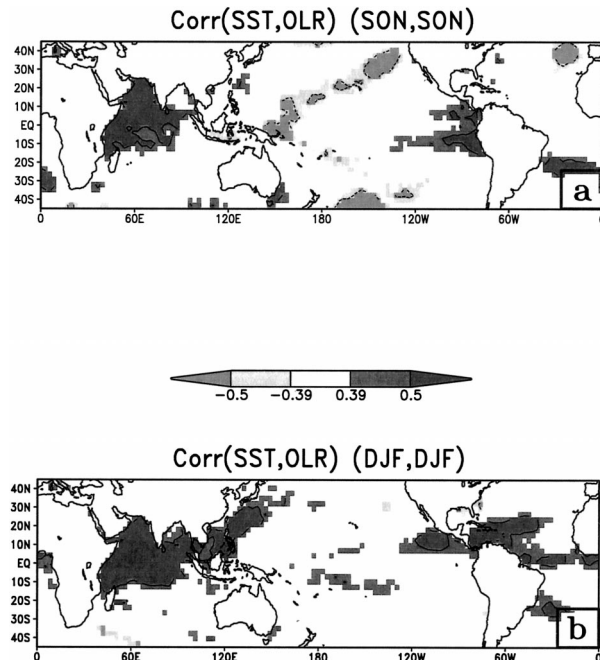


FIG. 7. Same as Fig. 5, but from experimental AGCM simulations.

ported by observations. Notwithstanding these errors in the AGCM, we can still glean some useful information from it.

A similar correlation plot was also made for the experimental AGCM runs that are shown in Fig. 7. It should be noted that these correlations have been computed with global observed SSTAs and the correlations appearing over the Pacific Ocean may therefore be regarded as noise. Unlike the control integration, the experimental runs display similar correlations over the WIO in both SON and DJF seasons. These results suggest that the influence of the WIO SSTAs, especially in DJF on OLR variability over the WPO at interannual time scales, is diminished in the presence of the SST variability over the Pacific Ocean. The correlations over the tropical Atlantic that appear in Fig. 7b are significant but not observed.

### c. Regression analysis

In this section I shall try to explain this teleconnection pattern from both the observations and the COLA AGCM simulations. The hypothesis for this teleconnection pattern is that the WIO SST is connected to the WPO OLR anomalies (a proxy to divergent circulations) through the east–west atmospheric equatorial circulation that is modulated by the underlying SST. To establish this hypothesis, I regressed the SSTAs for DJF over the WIO, the WPO, and the EPO separately with the equatorial zonal wind anomaly (EZWA) of DJF. In Figs. 8a–c, I show the vertical cross section of the contemporaneous response in the control AGCM integrations of

the EZWA to SSTAs of  $0.5^{\circ}$  over the WIO, the WPO, and the EPO from this derived linear relationship, respectively. It should be noted that significant values at a 90% confidence interval according to a  $t$  test are plotted. The control AGCM in Fig. 8a displays an easterly anomaly of the equatorial zonal wind (EZW) over the EPO region in the mid to upper troposphere in response to a positive SSTA over the WIO. Similarly, in Fig. 8b, in response to a positive SSTA over the EPO, an easterly EZWA with a much larger magnitude above 500 hPa develops in the control COLA AGCM simulation. Furthermore, the control run also shows a response of an easterly (westerly) anomaly in the lower troposphere over the WPO (EPO). In Fig. 8c we see that the response of EZW to SSTAs over the WPO is opposite in sign to the response to SSTAs over the EPO in Fig. 8b and is comparable in magnitude to the response to SSTAs over the WIO in Fig. 8a. In comparing these EZWAs with the model EZW climatology in Fig. 8d, we can discern that a positive SSTA over the EPO and the WIO diminishes the climatological Walker circulation over the equatorial Pacific Ocean, while a positive SSTA over the WPO acts to enhance it.

Similar figures derived from such linear regression equations from NCEP reanalysis EZW are plotted in Fig. 9. Although the responses are not identical, qualitatively they corroborate the response patterns obtained from the control COLA AGCM. In comparing the EZW climatology from the COLA AGCM (Fig. 8) with that from the NCEP reanalysis (Fig. 9), we can see that there are significant systematic errors such as the strong zonal wind in the lower troposphere displayed by the control model. This feature of the COLA AGCM is primarily on account of its erroneous feature of developing split ITCZs (Misra 2003) over the tropical Pacific, which implies a large deficit of precipitation and enhanced low-level winds over the equatorial Pacific region. In Fig. 10a the response pattern of EZWAs from the experimental AGCM run to SSTAs of  $0.5^{\circ}$  over the WIO is shown. The response in comparison to the control AGCM in Fig. 8a has clearly shifted westward. Furthermore, the influence of the WIO SSTAs on the EZW is in the lower troposphere, below 500 hPa. It should be noted that the EZW climatology in the experiment in Fig. 10b is comparable to the climatology displayed by the control in Fig. 8d. The response pattern in Fig. 10a suggests that there is a westward shift of the anomalous EZW circulation, resulting in a stronger influence of the WIO SSTAs to OLR variability over the WPO. A similar linear relationship was also seen in the SON season (not shown).

### d. A mechanistic explanation

A mechanistic explanation for this teleconnection from the aforementioned discussions is summarized in this section. Typically, under non-ENSO conditions the Walker circulation over the equatorial Pacific Ocean and

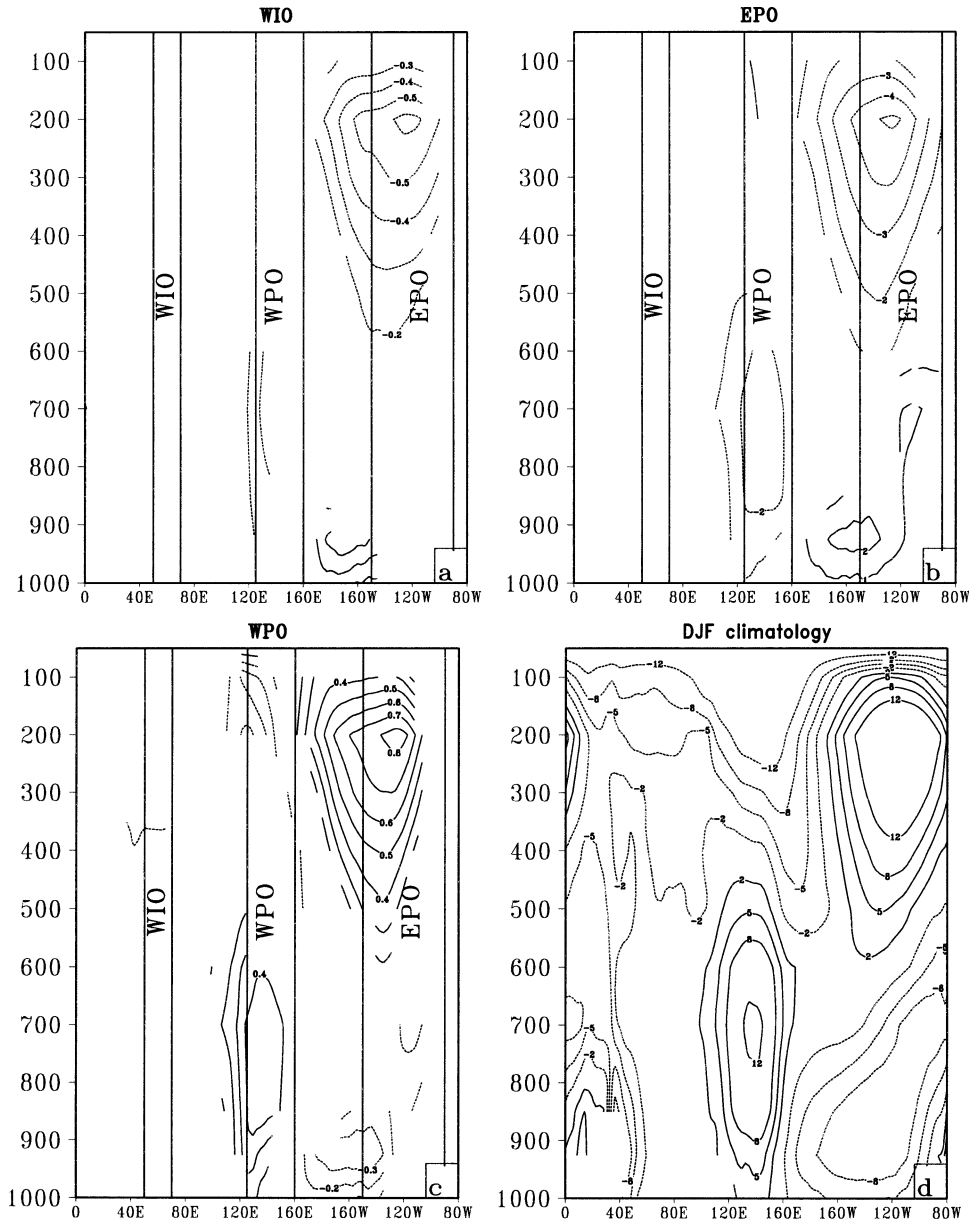


FIG. 8. The linear regression of SSTAs over the (a) WIO, (b) EPO, and (c) WPO on the control COLA AGCM zonal wind anomaly along the equator for the DJF season. The amplitude of the patterns corresponds to  $0.5^{\circ}$  SSTA. Only significant values at a 90% confidence interval according to a  $t$  test are plotted. (d) The climatological DJF equatorial zonal wind cross section from the control COLA AGCM. The units are in  $m s^{-1}$ .

EZW circulation over the Indian Ocean have their rising branches over a broad region of the western Pacific and eastern Indian Oceans, with their descending branches over a broad region of the western Pacific and eastern Indian Oceans, with their descending branches over the WIO and the EPO (Piexoto and Oort 1992), respectively. In the absence of the Pacific SST variability, an anomalous circulation develops that collocates the rising branch over the WIO and its descending branch over the WPO. This is best exemplified by Figs. 11a and 11b,

borrowed from Misra (2003), which show the mean DJF velocity potential and divergent wind at 200 hPa from the control run and its difference from the experimental run. The anomalous pattern observed in Fig. 11b clearly shows a broad region of upper-level divergence (convergence) over the Indian (Pacific) Ocean.

Many studies (Graham and Barnett 1987; Lau and Shen 1988; Betts and Ridgeway 1989) suggest that deep convection in the Tropics has a tendency to collocate over high SST ( $27^{\circ}$ – $28^{\circ}C$ ) regions. They allude to the

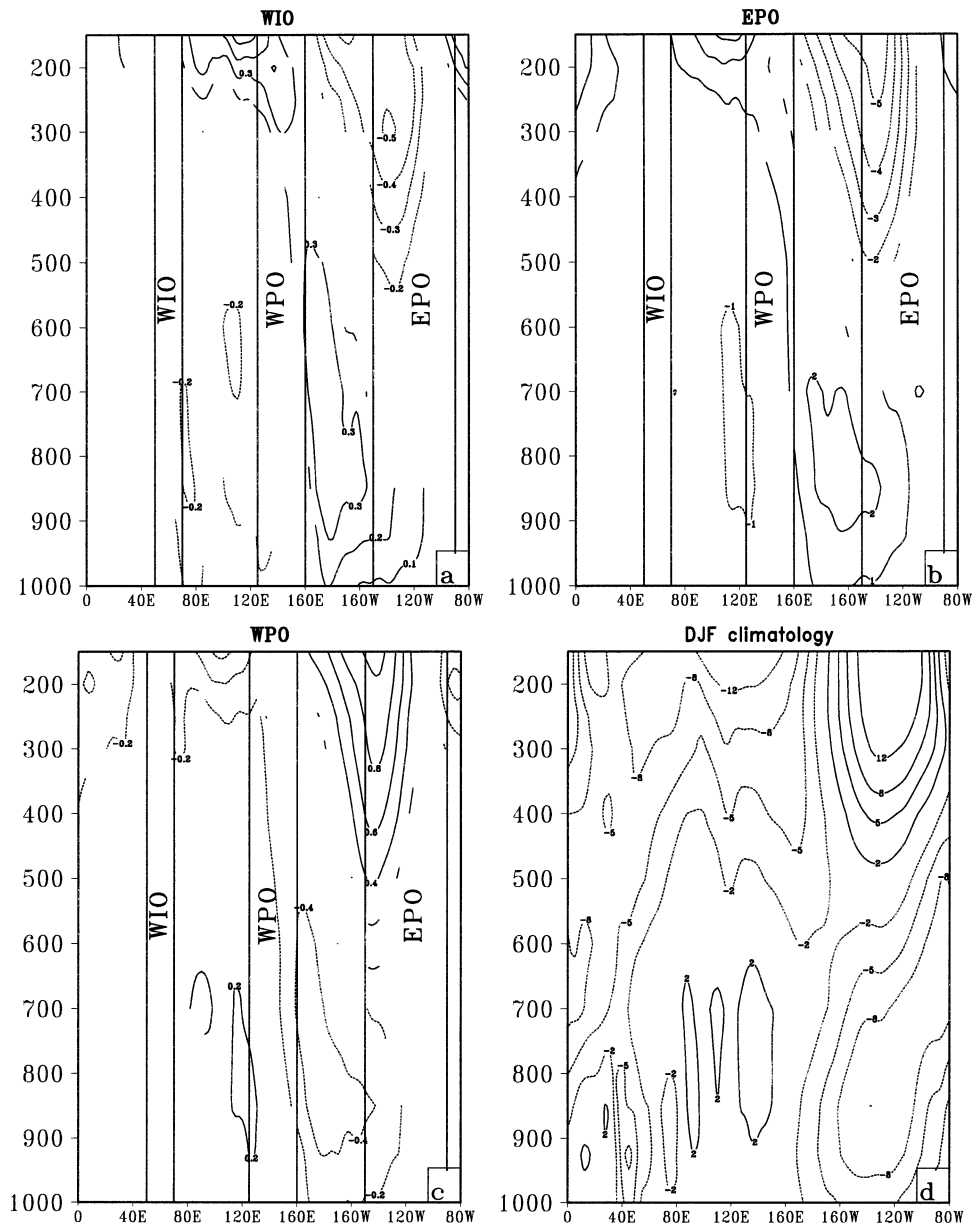


FIG. 9. Same as Fig. 8, but the equatorial zonal winds are from NCEP reanalysis.

fact that the surface temperature reaches a value at which the vertical stability of the atmosphere is sufficiently reduced to warrant the onset of large-scale moist convection. But in a related observational study of Waliser et al. (1993), it is shown that the amount and intensity of convection reduces in the deep Tropics when SST exceeds  $29.5^{\circ}\text{C}$ . Here, the argument is that very warm SSTs can occur only under diminished convection that otherwise reduces solar insolation due to the associated cloud systems and enhance surface fluxes of heat and moisture from the ocean surface.

In the experimental AGCM runs, the absence of SST variability over the Pacific Ocean reduces the intensity

of the EZW circulation. As a result, the influence of the Pacific SST on the variability of the OLR over the Indian Ocean also diminishes. It should also be noted that the SST over the WIO in SON and DJF from 1979 to 1996 remains, for the most part, in the range of  $27^{\circ}\text{--}29^{\circ}\text{C}$ . This results in enhanced local SSTA forcing on the OLR anomalies (deep convection) over the WIO in the experimental runs. This is shown in the time-longitude cross sections of OLR anomalies over the Indian Ocean from the control and experimental runs in Figs. 12a and 12b, respectively. In the experimental run (Fig. 12b), the negative OLR anomalies are largely confined to the WIO, while it is zonally oriented over the Indian Ocean

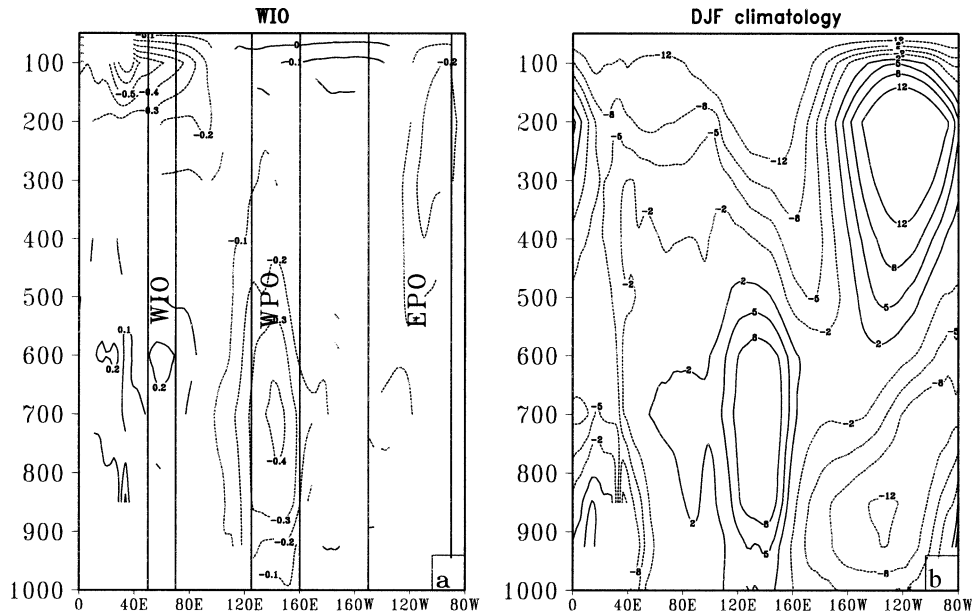
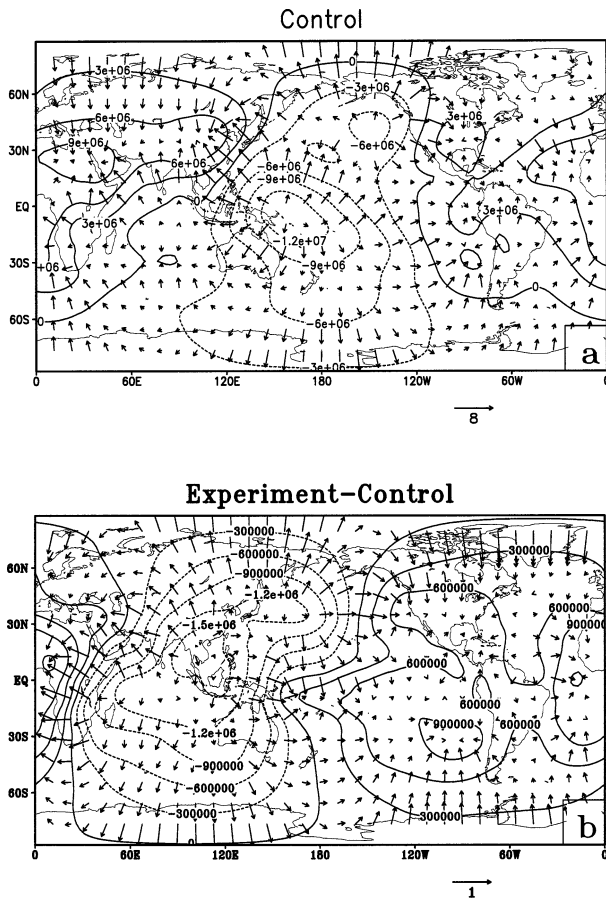


FIG. 10. (a) The linear regression of SSTAs over the WIO on an equatorial zonal wind anomaly from the experimental AGCM run for the DJF season. The amplitude of the patterns corresponds to a  $0.5^{\circ}$  SSTA over the WIO. Only significant values at a 90% confidence interval according to a  $t$  test are plotted. (b) The climatological equatorial zonal wind from the experimental AGCM runs are shown for the DJF season. The units are in  $\text{m s}^{-1}$ .



in the control integrations (Fig. 12a). Furthermore, the OLR anomalies in the experimental run over the WIO are stronger relative to the control run. A contemporaneous correlation of the OLR and SST anomalies for the DJF (SON) season over the WIO indicate a rise from  $-0.17$  ( $-0.40$ ) in the control run to  $-0.78$  ( $-0.57$ ) in the experimental run. The upper-level large-scale divergent circulations imposed by the enhanced convection over the WIO further diminish the intensity of the climatological equatorial east–west circulation in the experimental run.

#### 4. Conclusions

In this study I have shown that the western Indian Ocean (WIO) SST variability plays a critical role in the variability of the OLR anomaly over the western Pacific Ocean (WPO) at least over the two seasons of SON and DJF. I have used both AGCM simulations and observations to verify this relationship. The WPO OLR anomalies correlate positively with the WIO SSTAs in these teleconnection patterns in SON and DJF. In the absence of ENSO variability, the correlation over the WIO is further strengthened in the DJF season in the model

FIG. 11. (a) Velocity potential and divergent wind vectors at 200 hPa for DJF from the control mean. The isopleth interval is  $3.0 \times 10^6 \text{ m}^2 \text{ s}^{-1}$ . (b) The mean difference for DJF of velocity potential and divergent wind at 200 hPa between the control and experimental mean. The isopleth interval is  $3.0 \times 10^5 \text{ m}^2 \text{ s}^{-1}$ . The unit of the wind vectors is  $\text{m s}^{-1}$ . Figure borrowed from Misra (2003).

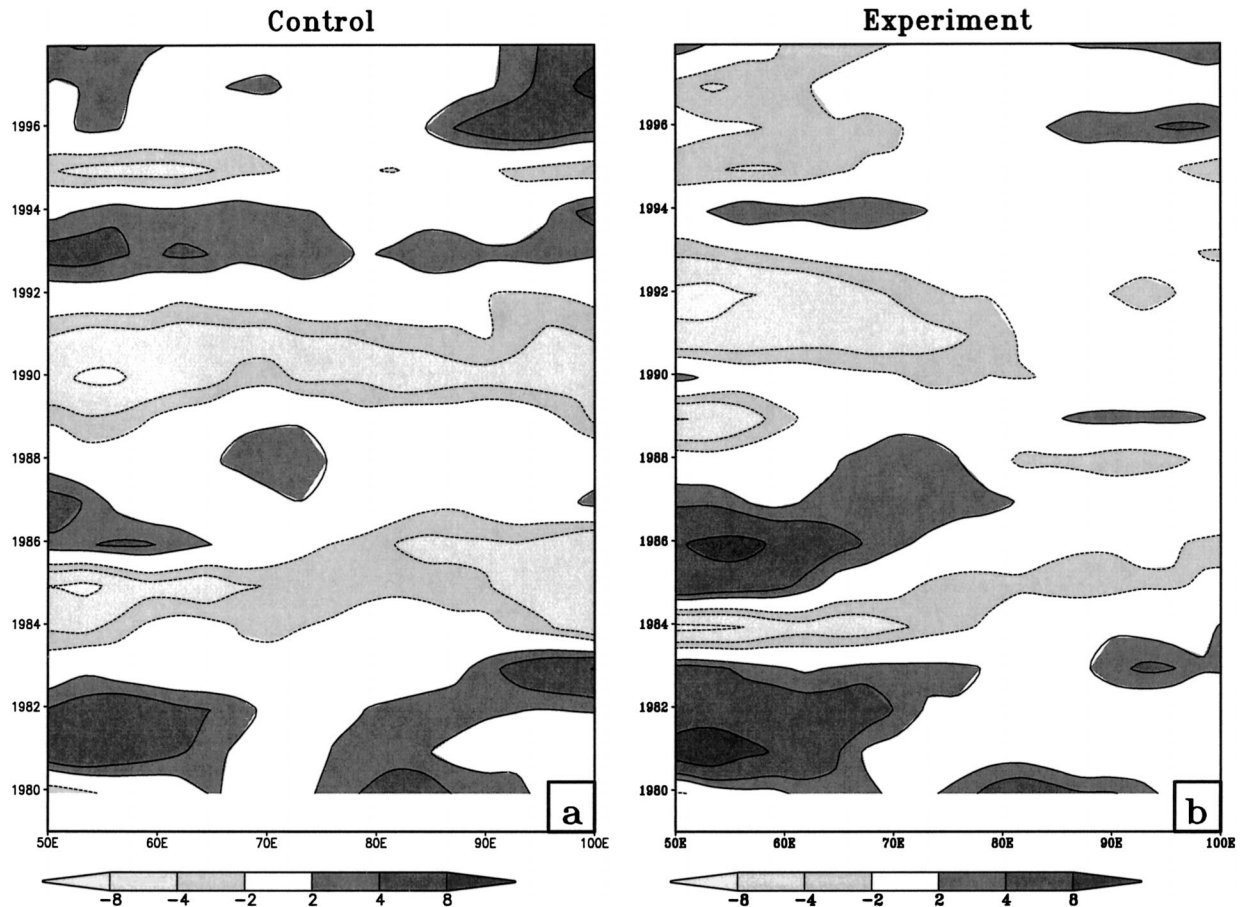


FIG. 12. The DJF OLR anomalies averaged between  $10^{\circ}\text{S}$  and  $10^{\circ}\text{N}$  from the (a) control and (b) experiment COLA AGCM integrations. The units are in  $\text{W m}^{-2}$ .

integrations. A regression analysis was performed to understand this teleconnection pattern both in observations and model integrations. The control AGCM shows that a positive SSTa over the EPO and the WIO acts to weaken the climatological Walker circulation over the Pacific Ocean. However, a positive SSTa over the WPO tends to strengthen the equatorial Walker circulation. It should be noted that the EZW response to SSTAs over the EPO is nearly an order of magnitude larger than the response to SSTAs over the other two regions. In the experimental run there is a westward shift of this response pattern to SSTAs over the WIO. This is associated with a westward shift of the increased deep convection over the WIO by enhanced modulation from the local SSTAs under a diminishing influence of the Walker circulation. The experimental run is therefore able to highlight the influence of the WIO SSTAs that are otherwise masked by the presence of the SST variability of the Pacific Ocean in the control run.

It should be noted that the results of this study have to be viewed with a caveat that no attempt has been made to explain the appearance of the SSTAs over the WIO. The use of an AGCM with prescribed SST may

be viewed as a limitation of this study to address the coupled ocean–atmosphere behavior.

*Acknowledgments.* I would like to thank Paul Dirmeier for providing the SST datasets for the experimental run and Ben Kirtman for his encouragement to pursue this study. The author also wishes to thank the three anonymous reviewers whose comments greatly improved the quality of the manuscript. This project was supported by NSF Grant ATM9814295, NASA Grant NAG5-11656, and NOAA Grant NA16GP2248.

#### REFERENCES

- Arpe, K., L. Dumenil, and M. A. Giorgetta, 1998: Variability in the Indian Monsoon in the ECHAM3 model: Sensitivity to sea surface temperature, soil moisture, and the stratospheric quasi-biennial oscillation. *J. Climate*, **11**, 1837–1858.
- Betts, A. K., and W. Ridgway, 1989: Climatic equilibrium of the atmospheric convective boundary layer over a tropical ocean. *J. Atmos. Sci.*, **46**, 2621–2641.
- Clark, C. O., J. E. Cole, and P. J. Webster, 2000: Indian Ocean SST and Indian summer rainfall: Predictive relationships and their decadal variability. *J. Climate*, **13**, 2503–2519.
- Curtis, S., G. J. Huffman, and R. F. Adler, 2002: Precipitation anom-

- alies in the tropical Indian Ocean and their relation to the initiation of El Niño. *Geophys. Res. Lett.*, **29**, 1441, doi:10.1029/2001GL013399.
- Davies, R., 1982: Documentation of the solar radiation parameterization in the GLAS climate model. NASA Tech. Memo. 83961, 57 pp.
- Dirmeyer, P. A., and F. J. Zeng, 1999: Precipitation infiltration in the simplified SiB land surface scheme. *J. Meteor. Soc. Japan*, **77**, 291–303.
- Fennessy, M. J., and Coauthors, 1994: The simulated Indian monsoon: A GCM sensitivity study. *J. Climate*, **7**, 33–43.
- Graham, N. E., and T. P. Barnett, 1987: Sea surface temperature, surface wind divergence, and convection over tropical oceans. *Science*, **238**, 657–659.
- Harshvardhan, R. Davies, D. A. Randall, and T. G. Corsetti, 1987: A fast radiation parameterization for atmospheric circulation models. *J. Geophys. Res.*, **92** (D1), 1009–1016.
- Huang, B., and J. L. Kinter, 2002: Interannual variability in the tropical Indian Ocean. *J. Geophys. Res.*, **107**, 3199, doi:10.1029/2001JCO01278.
- Kalnay, E., and Coauthors, 1996: The NCEP/NCAR 40-Year Reanalysis Project. *Bull. Amer. Meteor. Soc.*, **77**, 431–437.
- Kiehl, J. T., J. J. Hack, G. Bonan, B. A. Boville, D. L. Williamson, and P. J. Rasch, 1998: The National Center for Atmospheric Research Community Climate Model: CCM3. *J. Climate*, **11**, 1131–1149.
- Kirtman, B. P., and J. Shukla, 2000: Influence of the Indian summer monsoon on ENSO. *Quart. J. Roy. Meteor. Soc.*, **126**, 213–239.
- , D. A. Paolino, J. L. Kinter, and D. M. Straus, 2001: Impact of tropical subseasonal SST variability on seasonal mean climate simulations. *Mon. Wea. Rev.*, **129**, 853–868.
- , Y. Fan, and E. K. Schneider, 2002: The COLA global coupled and anomaly coupled ocean–atmosphere GCM. *J. Climate*, **15**, 2301–2320.
- Klein, S. A., B. J. Soden, and N. C. Lau, 1999: Remote sea surface temperature variations during ENSO: Evidence for a tropical atmospheric bridge. *J. Climate*, **12**, 917–932.
- Krishnamurthy, V., and B. P. Kirtman, 2001: Variability of the Indian Ocean: Relation to monsoon and ENSO. COLA Rep. 107, 39 pp. [Available from COLA, 4041 Powder Mill Rd., Suite 302, Calverton, MD 20705.]
- Lacis, A. A., and J. Hansen, 1974: A parameterization for the absorption of solar radiation in the earth's atmosphere. *J. Atmos. Sci.*, **31**, 118–133.
- Latif, M., and T. P. Barnett, 1995: Interactions of the tropical oceans. *J. Climate*, **8**, 952–968.
- , D. Dommenges, M. Dima, and A. Grotzner, 1999: The role of Indian Ocean sea surface temperature in forcing east African rainfall anomalies during December–January 1997/98. *J. Climate*, **12**, 3497–3504.
- Lau, K.-M., and S. Shen, 1988: On the dynamics of intraseasonal oscillations and ENSO. *J. Atmos. Sci.*, **45**, 1781–1797.
- Liebmann, B., and C. A. Smith, 1996: Description of a complete (interpolated) outgoing long-wave radiation dataset. *Bull. Amer. Meteor. Soc.*, **77**, 1275–1277.
- Makarau, A., and M. R. Jury, 1997: Predictability of Zimbabwe summer rainfall. *Int. J. Climatol.*, **17**, 1421–1432.
- Meehl, G. A., 1987: The annual cycle and interannual variability in the tropical Indian and Pacific Ocean regions. *Mon. Wea. Rev.*, **115**, 27–50.
- , 1993: A coupled air–sea biennial mechanism in the tropical Indian and Pacific Ocean regions. *J. Climate*, **6**, 31–41.
- , G. N. Kiladis, K. M. Weickmann, M. Wheeler, D. S. Gutzler, and G. P. Compo, 1996: Modulation of equatorial subseasonal convective episodes by tropical–extratropical interaction in the Indian and Pacific Ocean regions. *J. Geophys. Res.*, **101**, 15 033–15 049.
- Mellor, G. L., and T. Yamada, 1982: Development of a turbulence closure model for geophysical fluid processes. *Rev. Geophys. Space Phys.*, **20**, 851–875.
- Misra, V., 2003: The influence of Pacific SST variability on the precipitation over southern Africa. *J. Climate*, **16**, 2408–2418.
- Moorthi, S., and M. J. Suarez, 1992: Relaxed Arakawa–Schubert: A parameterization of moist convection for general circulation models. *Mon. Wea. Rev.*, **120**, 978–1002.
- Nicholls, N., 1989: Sea surface temperatures and Australian winter rainfall. *J. Climate*, **2**, 965–973.
- Nicholson, S. E., 1997: An analysis of the ENSO signal in the tropical Atlantic and western Indian Oceans. *Int. J. Climatol.*, **17**, 345–375.
- Parker, D. E., N. A. Rayner, E. B. Horton, and C. K. Folland, 1999: Development of the Hadley Center sea ice and sea surface temperature data sets (HADISST). Preprints, *WMO Workshop on Advances in Marine Climatology—CLIMAR99*, Vancouver, BC, Canada, WMO, 194–203. [Available from Environment Canada, 4905 Dufferin St., Downsview, ON M3H 5T4, Canada.]
- Piexoto, J. P., and A. H. Oort, 1992: *Physics of Climate*. American Institute of Physics, 520 pp.
- Shukla, J., 1987: Interannual variability of monsoons. *Monsoons*, J. S. Fein and P. L. Stephens, Eds., John Wiley, 399–463.
- Straus, D., and J. Shukla, 2002: Does ENSO force the PNA? *J. Climate*, **15**, 2340–2358.
- Tiedtke, M., 1984: The effect of penetrative cumulus convection on the large-scale flow in a general circulation model. *Beitr. Phys. Atmos.*, **57**, 216–239.
- Venzke, S., M. Latif, and A. Villwock, 2000: The couple GCM ECHO-2. Part II: Indian Ocean response to ENSO. *J. Climate*, **13**, 1371–1383.
- Waliser, D. E., N. E. Graham, and C. Gauthier, 1993: Comparison of the highly reflective cloud and outgoing longwave radiation datasets for use in estimating tropical deep convection. *J. Climate*, **6**, 331–353.
- Xue, Y.-K., P. J. Sellers, J. L. Kinter, and J. Shukla, 1991: A simplified biosphere model for global climate studies. *J. Climate*, **4**, 345–364.
- , F. J. Zeng, and C. A. Schlosser, 1996: SSiB and its sensitivity to soil properties: A case study using HAPEX–Mobilhy data. *Global Planet. Change*, **13**, 183–194.